# Acid-Triggered, Acid-Generating, and Self-Amplifying Degradable Polymers

Kali A. Miller,†¬¬,± Ephraim G. Morado,†,± Shampa R. Samanta,†,± Brittany A. Walker,†,± Arif Z. Nelson,§ Samya Sen,§ Dung T. Tran,† Daniel J. Whitaker,† Randy H. Ewoldt,§,∥ Paul V. Braun,†,‡,∥,¬ and Steven C. Zimmerman\*,†,∥

†Department of Chemistry, †Department of Materials Science and Engineering, §Department of Mechanical Science and Engineering, ¶Materials Research Laboratory, ¬Beckman Institute for Advanced Science and Technology, University of Illinois at Urbana-Champaign, Urbana, Illinois 61801, USA

### Supporting Information

**ABSTRACT:** We describe the 3-iodopropyl acetal moiety as a simple cleavable unit that undergoes acid catalyzed hydrolysis to liberate HI (pKa  $\sim$  -10) and acrolein stoichiometrically. Integrating this unit into linear and network polymers gives a class of macromolecules that undergo a new mechanism of degradation with an acid amplified, sigmoidal rate. This trigger-responsive self-amplified degradable polymer undergoes accelerated rate of degradation and agent release.

The simultaneous growth in waste plastics, 3D-printing, and implantable biomaterials has challenged chemists to develop new polymers able to meet the demands of real-world applications. In particular, there is increasing demand for smart polymers that change their shape or properties or degrade in response to environmental stimuli.<sup>1</sup>

Indeed, a renewed interest in degradable polymers, especially for biomedical and engineering applications has led to an extensive search for new mechanisms to breakdown polymers.<sup>2</sup> Most degradable polymers contain functional groups along their main chain that cleave independently by chemical or photochemical reaction, in which case, the degradation rate remains more or less constant until the trigger or cleavable functionality is consumed (Figure 1a). The discovery of self-immolative polymers was particularly exciting because one triggering event is sufficient to activate an entire polymer chain to degrade.<sup>3,4</sup> These systems are stable under ambient conditions until a reactive unit at the polymer end is cleaved, triggering a cascade of fragmentation reactions that proceed sequentially along the polymer chain (Figure 1b).

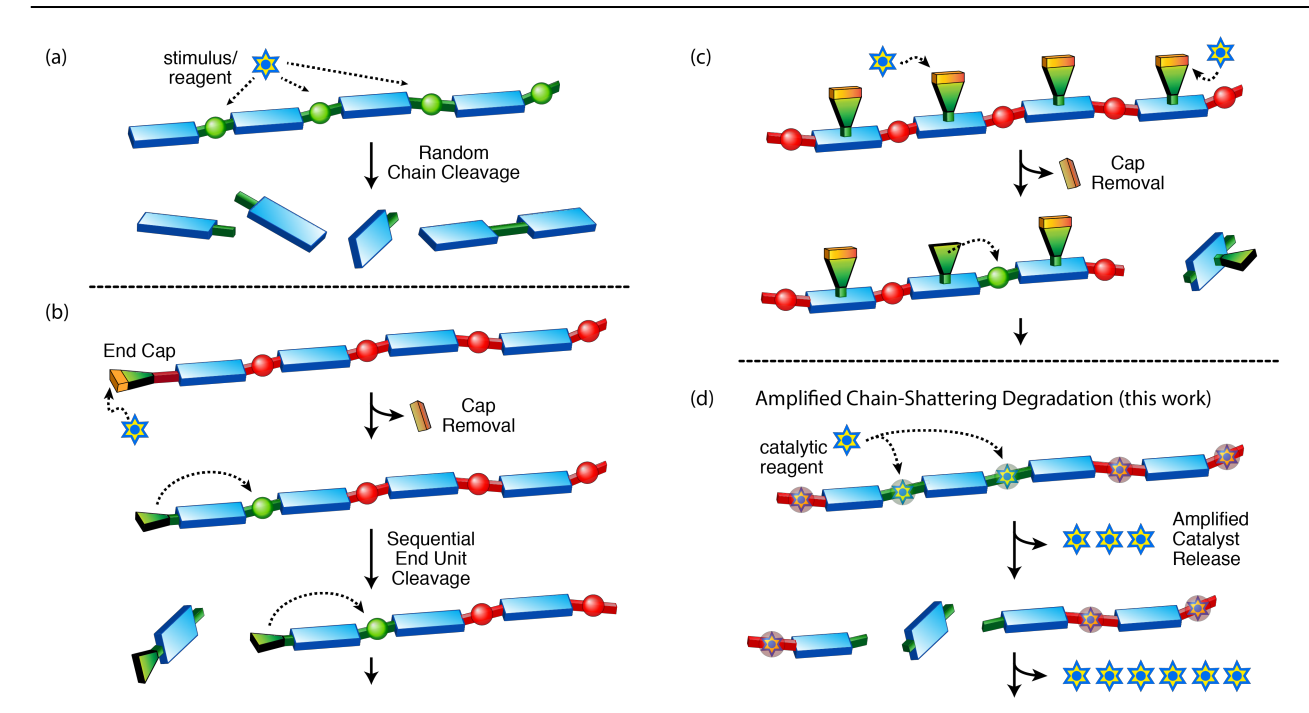


**Figure 1.** Schematic representation of polymer degradation mechanisms: (a) Traditional cleavage of polymer chain, (b) Self-immolative polymer degradation. Loss of end-cap is followed by sequential loss of end units, (c) Trigger-responsive chain-shattering polymer degradation mechanism, and (d) Amplified chain-shattering mechanism developed in the current work. Green linkages are labile under reaction conditions, whereas red are stable.

More recently, the development of chain-shattering polymers allows materials to spontaneously degrade along the main chain with a triggering event occurring at each monomer unit (Figure 1c).<sup>5</sup> Both the self-immolative and chain-shattering approaches do have limitations in degradation rate and require a stoichiometric amount of the triggering agent. We were interested in a less studied approach that can be referred to as an amplified chain-shattering degradation. In this mechanism, a catalytic species accelerates chain cleavage, which in turn generates a full equivalent of the same agent, leading to an exponential degradation cascade (Figure 1d).<sup>6</sup> For example, polyesters such as PLGA show mild autocatalysis because the liberated carboxylic acids accelerate the hydrolysis.<sup>7</sup>

Herein, we describe a simple, yet powerful acetal unit derived from 3-iodopropanal that undergoes acid catalyzed, self-amplified cleavage and demonstrate how it can be readily integrated into both degradable polymers and hydrogels. Unlike polyesters, our designed system shows strong autocatalysis and is more suitable to applications where exponential rates are needed. The acetal unit and acid trigger were chosen because pH gradients are ubiquitous in the environment and within biological systems. Furthermore, polymeric acetals (polyacetals) are well studied, with tunable reactivities and properties. The simplest, polyoxymethylene (POM) is a widely used engineering thermoplastic, whereas more complex polyacetals are used in a range of applications from controlled release to drug delivery.

The acetal design was based on small molecules reported by Ichimura and coworkers that produce p-toluenesulfonic acid (pKa  $\approx$  -2.8) in an amplified manner. With this starting point, various monomeric units were prepared and tested, ultimately leading to the 3-iodo-1,1-dialkoxy moiety as having the most suitable properties. In particular, this unit is easily prepared and has good stability, but undergoes acid amplified degradation under mildly acidic conditions. In this mechanism, the acetal likely hydrolyzes to the hemiacetal and then further to the aldehyde, which subsequently undergoes  $\beta$ -elimination to generate stoichiometric amounts of hydroiodic acid with pKa  $\approx$  -10 and acrolein (Scheme 1). Each of the three steps is catalyzed by acid.

## Scheme 1. Mechanism of 3-iodopropyl acetal hydrolysis with stoichiometric formation of HI and amplified cleavage.

$$H_2O$$
, cat.  $H^+$   $H_2O$ , cat.  $H^+$   $H^+$   $I^ I^+$   $I^+$   $I^$ 

The key 3-iodopropyl acetals **1-3** used in this study are shown in Scheme 2. The synthesis of iodo-acetal monomer **1** was achieved by treatment of acrolein with TMSBr and acetalization with alcohol **4** to afford **5**. <sup>10</sup> Conversion of bromo acetal **5** to the iodo acetal **1** proceeded in good yield under standard Finkelstein conditions. Iodo acetals **2** and **3** were prepared in analogous fashion or by using

Scheme 2

H O 1) TMSBr, PhH

2) HO O 4

TSOH, PhH, Dean-Stark; 54%

ADMET

ADME

ADMET

ADME

HCl in place of TMSBr, the diol units in **2** obtained by dihydroxylation (see Supporting Information).

3

2

The ability of the 3-iodopropyl acetal unit to undergo acid amplified cleavage was examined by monitoring the hydrolysis of  $\bf 3$  using  $^1H$  NMR under different conditions. A solution of  $\bf 3$  in  $D_2O$  at pD=5.5 at 70  $^{\circ}C$  showed an induction period of about 15-20 minutes at which time the acetal underwent a rapidly accelerating degradation (Figure 2a). The reaction was largely complete after about 45 min. Consecutive  $^1H$  NMR spectra taken over 1 h were consistent with the formation of hemiacetal  $\bf 7$ , further hydrolysis to aldehyde  $\bf 8$ , which subsequently undergoes  $\bf 6$ -elimination to generate hydroiodic acid (Figure 2b and Figure S1). The stoichiometric generation of the strong

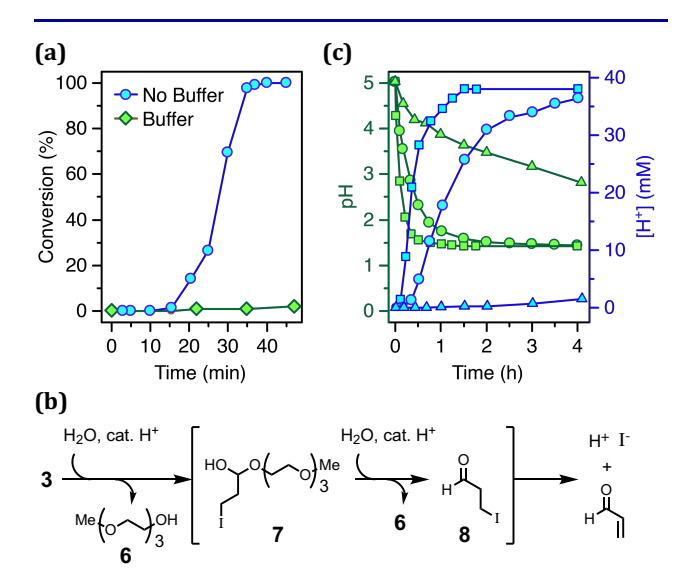


**Figure 2.** (a) Percent conversion of **3** in  $D_2O$  at initial pD = 5.5, with [**3**] = 48 mM at 70 °C in presence (green diamonds) and absence (blue circles) of 0.1 M acetate buffer. (b) Proposed mechanism of acetal hydrolysis with stoichiometric formation of HI and amplified cleavage. (c) Change in solution pH over time of a solution, [**3**] = 48 mM in nanopure water. Blue points, [H $^+$ ]; green points pH. Triangle, 50 °C, circle 70 °C, square, 90 °C. Connected lines are added to guide the eye.

acid HI can accelerate each of the previous steps and produce the nonlinearity observed for the process. Consistent with these observations, performing the same hydrolysis reaction in the presence of 0.1 M acetate buffer dramatically suppressed the hydrolysis rate as seen in Figure 2a.

The acid amplified degradation of **3** was further characterized by measuring the pH over time. Thus, 48 mM aqueous solutions of **3** in nanopure water, which was slightly acidic (pH = 5.5) due to dissolved atmospheric CO<sub>2</sub>, were heated at three temperatures (50, 70, and 90 °C) and the pH was measured at regular intervals (Figure 2c). The proliferation of acid was almost instantaneous at 90 °C, whereas an induction period of ca. 2 h and 5 min was observed at 50 °C and 70 °C, respectively. The release of acid at 50 °C could be made instantaneous by starting the reaction in a pH 3 solution by adding *p*-toluenesulfonic acid monohydrate. Both of the higher temperature reactions rapidly leveled off at pH  $\approx$  1.5, with the final [H+] value being consistent with near quantitative conversion of **3** to HI.

Final support for the autocatalytic, acid amplification mechanism comes from successfully fitting the degradation data of **3** at 70 °C to an autocatalytic kinetic model (Equation S1).<sup>11</sup> In this model, rate constants  $k_1$  and  $k_2$  describe the non-autocatalytic hydrolysis step and autocatalytic HI-accelerated steps, respectively. As expected for an autocatalytic reaction,  $k_1$  (1.9 x 10<sup>-4</sup> min<sup>-1</sup>)  $\ll k_2c_0$  (3.0 x 10<sup>-2</sup> min<sup>-1</sup>) (Table 1). Additional support for this model involves a linear fit of the data over time using Equation S3 and shown in Figure S6.

Table 1. Calculated rate constants for the non-autocatalytic and autocatalytic pathways of the degradation of 3, 10, and 13 at various temperatures. Average and standard deviation values are listed from three measurements.

	Temp (°C)	$k_1 (10^3  \text{min}^{-1})$	$k_2  (M^{-1} \text{min}^{-1})$
3	70	$0.19 \pm 0.26$	$6.2\pm1.2$
10	70	$0.16 \pm 0.19$	$2.9 \pm 0.6$
13	90	$37 \pm 6$	$7250\pm3810$

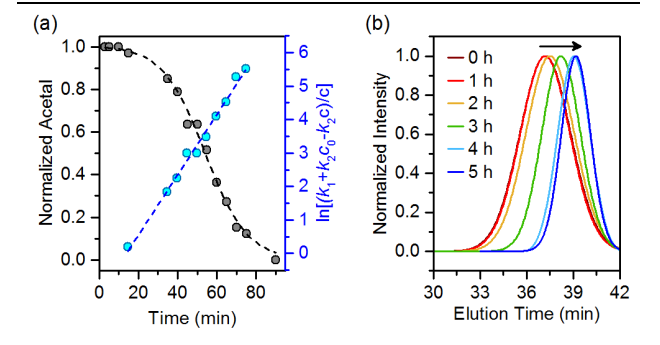


**Figure 3.** (a) Monitoring the disappearance of acetal functionality of  $\bf 10$  by  $^1H$  NMR as a 3 mM solution in  $D_2O/CD_3CN$  at  $70\,^{\circ}C$ . Dashed line is fit of the data to Equation S4 and dotted line is provided as a guide for the eye. (b) GPC traces of the degradation of  $\bf 10$  in a 0.3 M solution in  $H_2O/CH_3CN$  over time at  $70\,^{\circ}C$ .

Using Grubb's 1st generation catalyst, monomer 1 underwent successful acyclic diene metathesis (ADMET) polymerization providing polymer 9 with  $M_n \approx 10,000$ . Upjohn-dihydroxylation was subsequently used to convert 9 to 10 which significantly increased its water solubility (Scheme 2). However, polymer 10 exhibits thermoresponsiveness in pure aqueous solution with an LCST above room temperature. Therefore, a 40% (v/v) CD<sub>3</sub>CN in D<sub>2</sub>O (pD<sub>0</sub> = 5.5) mixture was used for degradation studies, which were monitored by  $^1$ H NMR spectroscopy and gel permeation chromatography (GPC).

The hydrolysis of  ${f 10}$  was observed in NMR by watching the disappearance of the acetal proton. A plot of normalized acetal conversion vs. time showed a distinctive sigmoidal shape that can be linearized (Figure 3a, Figure S7). This data fits well to our autocatalytic model and the extracted values for  ${f 10}$  agree with those observed for the degradation of  ${f 3}$  (Table 1). An autocatalytic, acid-amplified polymer degradation process should also be accompanied by a sigmoidal decrease in molar mass of  ${f 10}$ . As seen in Figure 3b, a solution of  ${f 10}$  heated to 70 °C was monitored at regular time intervals using GPC. Due to self-amplified degradation, there are only small changes in the

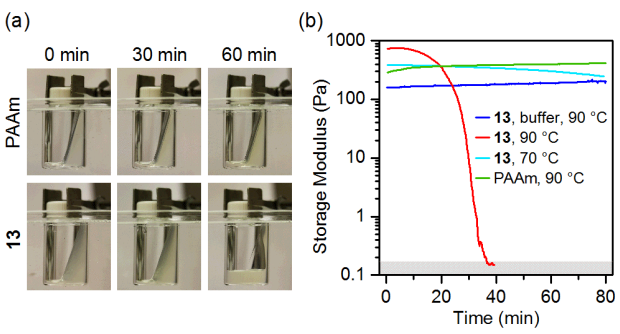


**Figure 4.** (a) Visual observation of the degradation of **13** compared to polyacrylamide control at 90 °C. Pictures are of the gel in a scintillation vial submerged in an oil bath. (b) Storage modulus of **13** at 70 °C, **13** with and without 0.1 M acetate buffer at 90 °C, and the polyacrylamide hydrogel at 90 °C.

GPC traces at first, followed by a rapid increase in retention time, and then much smaller changes.

Upon successful demonstration of the acid triggered self-amplified degradation behavior of the small molecule and linear polymer, we were interested in developing a degradable hydrogel containing the 3-iodopropyl acetal moiety. Treatment of 1 with HCl and acetalization with TMS-protected *N*-hydroxyethyl acrylamide gave 11, which was converted to acrylamide crosslinker 12 containing a central 3-iodopropyl acetal unit. Finally, degradable hydrogel 13 was synthesized by free radical polymerization using 3 mol% of 12 as the crosslinker and the monomer acrylamide (AAm) with diethoxyacetophenone (DEAP) as the photo-initiator (Scheme 3 and S6). An additional example of polyol hydrogel synthesis and visual observation of its degradation can be found in the Supplemental Information.

Scheme 3. Synthesis of degradable hydrogel 13.

Hydrogel 13 was studied and compared to gels prepared with a nondegradable crosslinker (N,N'-methylenebisacrylamide) in the same mole ratio (Scheme S7). Visual observation of hydrogel degradation over time shows that 13 has a delay period of ~30 min and then degrades rapidly to give a solution, whereas the polyacrylamide control did not show any sign of degradation (Figure 4a). The degradation process was also characterized using rheology. The storage modulus was measured, and minimal degradation was seen from the polyacrylamide control (PAAm) at 90 °C, 13 at 70 °C, and 13 at 90 °C in 0.1 M acetate buffer. However, upon heating to 90 °C, 13 undergoes the rapid degradation that is characteristic of autocatalytic reactions (Figure 4b). This degradation profile was quantified using the autocatalytic rate equations described above and in the Supporting Information, including an interrelation between elastic modulus and concentration to compare the apparent chemical rate constants (Figure S8). The increase of  $k_1$  and  $k_2$  for 13 can be attributed to increased hydrolysis and amplification rates at higher temperatures (Table 1).

In conclusion, we demonstrated a novel class of triggerresponsive self-amplified-degradable materials. The specific moiety developed here, the 3-iodopropyl acetal group, produces two products stoichiometrically: (1) hydroiodic acid, a very strong acid that accelerates further degradation, and (2) acrolein, a potent biocide and mercaptan scavenger. We anticipate that this acid amplifying motif could serve as a unique method for the controlled delivery of protic acid for various biological and chemical applications. These materials may also serve as benign carriers that undergo amplified release of biocidal acrolein in acidic solution. Investigations in these directions are currently in progress in our laboratory. We are further developing polymers for the self-amplified release of other reagents as well as other architectures with different rates and byproducts to expand the toolbox for potential applications.

#### ASSOCIATED CONTENT

**Supporting Information** 

The Supporting Information is available free of charge on the ACS Publications website.

Detailed experimental procedures, NMR spectra, additional characterization and kinetic data, kinetic modeling details, and synthesis and degradation of a PEG-based hydrogel (PDF)

#### **AUTHOR INFORMATION**

#### **Corresponding Author**

\*sczimmer@illinois.edu

#### **ORCID**

Kali A. Miller: 0000-0003-3632-0615 Randy H. Ewoldt: 0000-0003-2720-9712 Paul V. Braun: 0000-0003-4079-8160

Steven C. Zimmerman: 0000-0002-5333-3437

#### **Author Contributions**

<sup>⊥</sup>K.A.M., E.G.M, S.R.S., and B.A.W contributed equally.

#### Notes

The authors declare no competing financial interest.

#### ACKNOWLEDGMENT

The authors gratefully acknowledge support from the Dow Chemical Company, the National Science Foundation (NSF CHE-1709718), the Department of Defense/US Army W911NF-17-1-0351, and the US Department of Energy, Office of Science, Basic Energy Sciences (DE-FG02-07ER46471). K.A.S. acknowledges the National Science Foundation for support (DGE-1746047). We thank Shuqi Lai, Eric S. Epstein, Kaitlyn Curtis, Hsuan-Chin Wang, and Yugang Bai for technical support and insightful discussions.

#### **REFERENCES**

- (1) For lead reviews of stimuli responsive polymers see: (a) Stuart, M. A. C.; Huck, W. T. S.; Genzer, J.; Muller, M.; Ober, C.; Stamm, M.; Sukhorukov, G. B.; Szleifer, I.; Tsukruk, V. V.; Urban, M.; Winnik, F.; Zauscher, S.; Luzinov, I.; Minko, S. *Nat. Mater.* **2010**, *9*, 101-113. (b) Fomina, N.; Sankaranarayanan, J.; Almutairi, A. *Adv. Drug Deliver. Rev.* **2012**, *64*, 1005-1020. (c) Yan, X. Z.; Wang, F.; Zheng, B.; Huang, F. H. *Chem. Soc. Rev.* **2012**, *41*, 6042-6065. (d) Roy, D.; Brooks, W. L. A.; Sumerlin, B. S. *Chem. Soc. Rev.* **2013**, *42*, 7214-7243. (e) Schattling, P.; Jochum, F. D.; Theato, P. *Polym. Chem.* **2014**, *5*, 25-36. (f) Lehn, J. M. *Angew. Chem. Int. Ed.* **2015**, *54*, 3276-3289. (g) Wei, M. L.; Gao, Y. F.; Li, X.; Serpe, M. J. *Polym. Chem.* **2017**, *8*, 127-143.
- (2) For recent reviews of degradable polymers see: (a) Binauld, S.; Stenzel, M. H. *Chem. Commun.* **2013**, 49, 2082-2102. (b) Delplace, V.; Nicolas, J. *Nat. Chem.* **2015**, 7, 771-784. (c) Kamaly, N.; Yameen, B.; Wu, J.; Farokhzad, O. C. *Chem. Rev.* **2016**, 116, 2602-2663. (d) Albertsson, A. C.; Hakkarainen, M. *Science* **2017**, 358, 872-873.
- (3) (a) Li, S.; Szalai, M. L.; Kevwitch, R. M.; McGrath, D. V. *J. Am. Chem. Soc.* **2003**, *125*, 10516-10517. (b) de Groot, F. M. H.; Albrecht, C.; Koekkoek, R.; Beusker, P. H.; Scheeren, H. W. *Angew. Chem. Int. Edit.* **2003**, *42*, 4490-4494. (c) Amir, R. J.; Pessah, N.; Shamis, M.; Shabat, D., *Angew. Chem. Int. Edit.* **2003**, *42*, 4494-4499.
- (4) (a) Peterson, G. I.; Larsen, M. B.; Boydston, A. J. *Macromolecules* **2012**, *45*, 7317-7328. (b) Wong, A. D.; DeWit, M. A.; Gillies, E. R. *Adv. Drug Deliver. Rev.* **2012**, *64*, 1031-1045. (c) Wang, H. C.; Zhang, Y. F.; Possanza, C. M.; Zimmerman, S. C.; Cheng, J. J.; Moore,

- J. S.; Harris, K.; Katz, J. S. ACS Appl. Mater. Inter. **2015**, 7, 6369-6382.
- (5) (a) Zhang, Y. F.; Yin, Q.; Yin, L. C.; Ma, L.; Tang, L.; Cheng, J. J. *Angew. Chem. Int. Edit.* **2013**, *52*, 6435-6439. (b) Mutlu, H.; Barner-Kowollik, C. *Polym. Chem.* **2016**, *7*, 2272-2279.
- (6) For related self-propagating amplification reaction systems in sensing using small molecules and dendrimers, see: (a) Sella, E.; Shabat, D. *J. Am. Chem. Soc.* **2009**, *131*, 9934-9936. (b) Mohapatra, H.; Kim, H.; Phillips, S. T. *J. Am. Chem. Soc.* **2015**, *137*, 12498-12501. (c) Sung, X. L.; Dahlhauser, S. D.; Anslyn, E. V. *J. Am. Chem. Soc.* **2017**, *139*, 4635-4638. (d) Sun, X.; Shabat, D.; Phillips, S. T.; Anslyn, E. V. *J. Phys. Org. Chem.* **2018**, e3827.
- (7) (a) Siepmann, J.; Elkharraz, K.; Siepmann, F.; Klose, D., *Biomacromolecules* **2005**, *6*, 2312-2319. (b) Versypt, A. N. F.; Pack, D. W.; Braatz, R. D. *J. Control. Release* **2013**, *165*, 29-37.
- (8) (a) Masamoto, J. *Progr. Polym. Sci.* **1993**, *18*, 1-84. (b) Murthy, N.; Thng, Y. X.; Schuck, S.; Xu, M. C.; Frechet, J. M. J. *J. Am. Chem. Soc.* **2002**, *124*, 12398-12399. (c) Visakh, P. M., and Sarath

- Chandran. *Polyoxymethylene Handbook: Structure, Properties, Applications and Their Nanocomposites.* John Wiley & Sons, 2014. (d) Fan, B.; Trant, J. F.; Wong, A. D.; Gillies, E. R. *J. Am. Chem. Soc.* **2014**, *136*, 10116-10123. (e) Kaitz, J. A., Lee, O. P. and Moore, J. S. *MRS Commun.* **2015**, *5*, 191-204. (f) Liu, B.; Thayumanavan, S. *J. Am. Chem. Soc.* **2017**, *139*, 2306-2317.
- (9) (a) Arimitsu, K.; Kudo, K.; Ichimura, K. *J. Am. Chem. Soc.* **1998**, *120*, 37-45. (b) Ichimura, K. *Chem. Rec.* **2002**, *2*, 46-55.
- (10) (a) Hsung, R. P. *Synth. Commun.* **1990**, *20*, 1175-1179. (b) Paquette, L. A.; Tae, J. *J. Org. Chem.* **1996**, *61*, 7860-7866.
- (11) (a) Mata-Perez, F.; Perez-Benito, J. F. *J. Chem. Educ.* **1987**, 64, 925-927. (b) Perez-Benito, J. F. *J. Phys. Chem. A* **2011**, 115, 9876-9885. (c) Lee, O. P.; Hernandez, H. L.; Moore, J. S. *ACS Macro Lett.* **2015**, 4, 665-668. (d) Ashley, B.; Vakil, P. N.; Dyer, C. M.; Tracy, J. B.; Owens, J.; Strouse, G.F. *ACS Nano* **2017**, 11, 9957-9967.

## Insert Table of Contents artwork:

